The *Deinococcus radiodurans*-Encoded HU Protein Has Two DNA-Binding Domains†

Sharmistha Ghosh‡ and Anne Grove*

Department of Biological Sciences, Louisiana State University, Baton Rouge, Louisiana 70803

Received July 18, 2005; Revised Manuscript Received December 7, 2005

ABSTRACT: *Deinococcus radiodurans* can reconstitute its genome from double-strand breaks, most likely due to unusually efficient DNA repair and recombination. Factors that may contribute to such processes include the histone-like protein HU. The *D. radiodurans*-encoded HU (DrHU), which binds preferentially to DNA recombination intermediates, contains a 47-amino acid extension preceding the fold characteristic of HU proteins. Here we use electrophoretic mobility shift assays and DNA footprinting to show that the DrHU N-terminal domain significantly modulates DNA binding. The truncated DrHU (ΔDrHU), comprising only the conserved DNA-binding fold, has a site size of ∼11 bp in contrast to full-length DrHU which does not stably engage DNA shorter than ∼50 bp. Unlike wild-type DrHU, ΔDrHU distinguishes between linear DNA and DNA with nicks or gaps. ΔDrHU also binds preferentially to four-way junction (4WJ) DNA, with half-maximal saturation of 1.4 ± 0.4 nM compared to 20 ± 2 nM for 37 bp duplex DNA. However, in contrast to full-length protein which binds the junction arms, ΔDrHU primarily protects the junction crossover. Evidently, the DrHU N-terminus changes the mode of binding to both 4WJ DNA, duplex DNA, and DNA with nicks or gaps, thereby resulting in DrHU binding preferentially only to 4WJ structures. Combined with Western blots that confirm the presence of the extended form of DrHU in vivo, our data provide mechanistic insight into discrimination between 4WJ DNA and other distorted DNA constructs and suggest that an in vivo role of DrHU may be to stabilize DNA junctions.

HU[1] proteins are ubiquitous in prokaryotes, and they are abundant (*1*−*3*). These dimeric proteins are structurally conserved, with α-helices intertwining to form a compact body, from which *β*-sheets extend to encircle the DNA (*4*−*6*). The structures of *Escherichia coli* integration host factor (IHF) and *Anabaena* HU in complex with DNA show that two prolines intercalate into the DNA base-pair stack, forming two DNA kinks. While an ∼160° bend is induced by IHF, *Anabaena* HU introduces a variable DNA bend of 105−140° (*7, 8*).

In *E. coli*, HU functions primarily as an architectural protein. It binds double-stranded DNA nonspecifically and with low affinity and with considerably higher affinity (nM) for distorted DNA, including DNA with nicks, gaps, or mismatches. *E. coli* HU participates in DNA compaction by bending the DNA and constraining negative supercoils, and it plays a role in transcriptional regulation, Mu transposition, and DNA replication (*9*−*19*). Cells lacking HU are highly sensitive to *γ* and UV irradiation, suggesting its role in DNA repair and recombination (*18*−*21*).

Deinococcus radiodurans is one of 11 characterized members of the family *Deinococcaceae*, best known for its remarkable capacity to survive the effects of double-strand DNA breaks incurred, for example, upon exposure to ionizing radiation or prolonged desiccation (*22*, *23*). It can reconstitute its genomic DNA from 1000 to 2000 double-strand breaks, whereas an excess of 10−15 double-strand breaks is lethal to *E. coli* (for a review, see ref *24*). *D. radiodurans* has multiple genome equivalents, and it has been suggested that efficient homologous recombination may be a contributing factor to the damage resistance (*25*−*28*).

D. radiodurans HU (DrHU) has unique DNA-binding properties (*29*). While DNA-binding site sizes for HU homologues vary, from ∼37 bp for *E. coli* IHF and *Thermotoga maritima* HU, to an optimal binding site of ∼19 bp for *Anabaena* and *Helicobacter pylori* HU and a much shorter DNA binding site of ∼9 bp for *E. coli* HU, we have recently shown that stable complex formation with DrHU requires DNA longer than ∼50 bp (*7*, *8*, *13*, *29*−*32*). DrHU also has a distinct preference for four-way DNA junctions compared to linear double-stranded DNA: DrHU binds to the junction arms, while leaving the crossover exposed. This is in contrast to *E. coli* HU, which was shown to protect primarily the junction crossover (*12*).

DrHU has a 47 amino acid N-terminal extension, followed by the conserved type II DNA-binding fold that defines HU proteins. We show here that DrHU truncated for its N-terminal domain (ΔDrHU) binds to double-stranded DNA with a binding site size of only ∼11 bp, indicating that the

† Supported by the National Science Foundation (MCB-0414875 to A.G.).

* Corresponding author. Tel: 225-578-5148. Fax: 225-578-8790. Email address: agrove@lsu.edu.

‡ Current Address: Department of Biological Chemistry and Molecular Pharmacology, Harvard Medical School, Boston, MA.

[1] Abbreviations: DrHU, *Deinococcus radiodurans* HU; ΔDrHU, DrHU deleted for its N-terminal extension; HBsu, *Bacillus subtilis* HU; EMSA, electrophoretic mobility shift assay; CD, circular dichroism; T_m, melting temperature; 4WJ, four-way junction.

10.1021/bi0514010 CCC: $33.50
Published on Web 01/20/2006

N-terminal domain prevents stable interaction with shorter DNA duplexes. While ΔDrHU also binds preferentially to four-way junction (4WJ) DNA, the absence of the N-terminal domain changes the mode of binding to the DNA, with ΔDrHU protecting mainly the junction crossover. Our data indicate that the DrHU N-terminal domain serves to attenuate the mode of DNA interaction that is characteristic of HU proteins and provide mechanistic insight into the discrimination between 4WJ DNA and other distorted DNA constructs. We propose that DrHU may play a regulatory role in DNA recombination by stabilizing 4WJ DNA.

MATERIALS AND METHODS

Cloning, Overexpression, and Purification of ΔDrHU. The gene encoding ΔDrHU was amplified from plasmid pET-DrHU (*29*) with primers ΔDrHU-up (5′-GCTCTATC-CCCATATGCCCCCCTTCACAGC-3′) encoding a methionine at the 48th amino acid instead of lysine and a reverse primer ΔDrHU-down (5′-CGGAGGGAGCGGTCACATAT-GAACCCGCTTACAGG-3′), which was positioned at the start site of the DrHU gene and reading into the plasmid pET5a. PCR product with NdeI sites at both ends (as indicated with underlines) was digested and ligated with T4 DNA ligase to form plasmid pET5a-ΔDrHU. Integrity of the plasmid was confirmed by sequencing. The plasmid was transformed into *E. coli* BL21(DE3)pLysS and protein expression induced with 1 mM IPTG at $OD_{600} = 0.3$. Cell were harvested 2 h after induction and stored at −80 °C.

Purification of ΔDrHU was carried out at 0−4 °C. Cells were resuspended in lysis buffer (*29*) and lysed by sonication. The cell lysate was fractionated by ammonium sulfate precipitation, as described (*33*). The precipitate formed with 75% $(NH_4)_2SO_4$ was collected, dissolved in buffer A (20 mM Tris-HCl (pH 7.0), 50 mM KCl, 5% glycerol, 1 mM Na_2-EDTA, 3.5 mM 2-mercaptoethanol, and 0.2 mM phenyl methyl sulfonyl fluoride (PMSF)), dialyzed against buffer A, and applied to a preequilibrated CM sepharose column. Protein was eluted with a linear gradient from 50 mM to 1 M KCl in buffer A. Peak fractions were adjusted to 50% saturation with $(NH_4)_2SO_4$ and loaded on a phenyl sepharose column equilibrated in buffer A containing 50% $(NH_4)_2SO_4$. ΔDrHU was eluted with a linear gradient from 50 to 0% $(NH_4)_2SO_4$. Peak fractions were pooled and dialyzed against buffer A and loaded on a hydroxyapatite column equilibrated with buffer A, and eluted as described for the CM-sepharose column. Peak fractions were pooled and dialyzed in buffer A and applied to a heparin-sepharose column, and eluted as described for the CM-sepharose column. Purity was ascertained by Coomassie staining of gels overloaded with protein. Concentrations of both full-length and truncated DrHU were determined by Coomassie blue stained SDS−polyacrylamide gels, using BSA as a standard (although this approach may lead to some systematic error due to possible unequal staining of different proteins), as ΔDrHU contains neither tyrosine or tryptophan. Stain intensity was quantified using an AlphaImager and software provided by the manufacturer (Alpha Innotech). Glutaraldehyde-mediated cross-linking of ΔDrHU was performed as described (*29*).

Western Blotting. DrHU and ΔDrHU were electrophoresed on a 10% SDS−PAGE gel and transferred to a nitrocellulose membrane at 100 V for 2 h. The membrane was blocked for nonspecific binding using 5% nonfat milk in 1× phosphate buffered saline with 0.1% Tween-20 (PBST) for 1 h. The membrane was incubated for 1 h with mouse monoclonal anti-histone H1 antibody (*34*), generously provided by P. DiMario, followed by incubation with secondary antibody anti-mouse-IgG for 1 h and incubation with a colorimetric substrate, Opti-4CN (BioRad). Each step was preceded by two washes in 1× PBST buffer. The anti-histone H1 antibody was purified from culture supernatants using protein G (Sigma). The supernatant was incubated with protein G-agarose beads in 20 mM sodium phosphate buffer, pH 7.0, washed and eluted with 100 mM glycine HCl, pH 2.7. Equal amounts of 1 M Tris, pH 8.0 was added to raise the pH of the antibody, which was stored at −80 °C.

D. radiodurans cell lysates were isolated from cultures grown at 30 °C for 48 h. Cell pellets were stored at −80 °C, resuspended in buffer A, sonicated, and the lysate was centrifuged at 15000*g* for 20 min. The supernatant was dialyzed against buffer A, and aliquots were stored at −80 °C.

Circular Dichroism Spectroscopy. Circular dichroism (CD) spectra were recorded as described (*31*). The protein concentration was 0.1 mg/mL in 10 mM sodium phosphate buffer pH 7.0 with 50 mM NaCl. For thermal denaturation, spectra were recorded from 190 to 250 nm with 1 nm increments at each temperature, using a protein concentration of 0.025 mg/mL. Data were collected from 5 to 90 °C in 5° intervals. CD signals at 218, 219, 220, and 221 nm was used for analyses of thermal denaturation curves which were fit to modified van't Hoff equation for two-state unfolding from 25 to 90 °C (*35*):

$$\Delta\theta = ((m_n T + b_n) + (m_d{*}T + b_d)){*}K/(1+K) \text{ and}$$
$$K = \exp((-\Delta H°(1 - T/T_m))/RT)$$

where $\Delta\theta$ is molar ellipticity, m_n and b_n are the slope and intercept of the native state, m_d and b_d are the slope and intercept of the denatured state, T is the temperature in Kelvin, T_m is the melting temperature, $\Delta H°$ is the van't Hoff enthalpy, and R is the gas constant. Data were fitted using KaleidaGraph.

Electrophoretic Mobility Shift Assays. Electrophoretic mobility shift assays (EMSA) were performed using 8% (w/v) polyacrylamide gels (39:1(w/w) acrylamide:bisacrylamide) in TBE (45 mM Tris-borate pH 8.3, 1 mM EDTA). Gels were prerun for 30 min at 20 mA at room temperature before loading the samples with the power on. Reaction conditions were as described (*29*): 20 mM Tris pH 8.0, 10 mM $MgCl_2$, 50 mM NaCl, 0.1 mM Na_2EDTA, 0.1 mM DTT, 0.05% Brij58, 100 μg/mL BSA, and each sample contained 100 fmol of DNA in a total reaction volume of 10 μL, unless otherwise noted. DNA concentrations were determined from the absorbance at 260 nm, using the calculated extinction coefficient for each oligonucleotide. One strand of each DNA construct was then 5′-end ^{32}P-labeled with T4 polynucleotide kinase, and DNA constructs were annealed by combining 90% unlabeled oligonucleotide with 10% of the corresponding labeled material prior to mixing with stoichiometric amounts of the complementary unlabeled DNA strand(s) and heating to 90 °C, followed by slow cooling to room temperature. The presence of all strands in nicked or gapped

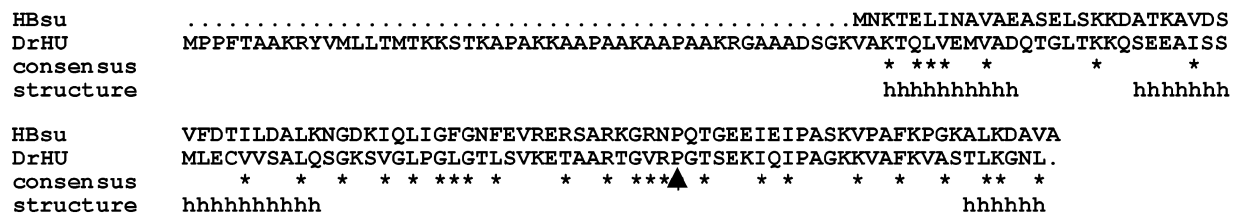

FIGURE 1: Sequence alignment of DrHU and *B. subtilis* HU (HBsu), derived from a ClustalX alignment of 60 HU homologues (*30*). Conserved residues are identified by asterisks. Helical segments are indicated below the alignment (h), and the DNA-intercalating proline is identified by an arrow.

constructs was confirmed by observing a change in mobility compared to partially annealed DNA.

Binding isotherms were analyzed using nonlinear fits of DNA titrated with protein, using the Hill equation $f = f_{max}[HU]_f^n/(K_d^n + [HU]_f^n)$ where $[HU]_f$ is the free protein concentration, f is fractional saturation, K_d represents the aggregate affinity for the DNA probe, n is the Hill coefficient, and f_{max} represents maximal saturation (included primarily to account for any complex dissociation during electrophoresis). Note that the aggregate affinities do not reflect actual binding constants for the reactions composed of several equilibria, each characterized by individual binding constants, and are only semiquantitative comparisons. Fits were performed using the program KaleidaGraph, and quality of the fits was evaluated by visual inspection, χ^2 values and correlation coefficients. The nonspecific binding site size was calculated from titrations under stoichiometric conditions ([DNA] > K_d) (*31*). The fraction of active ΔDrHU was calculated from stoichiometric titrations of 0.5 μM ΔDrHU with increasing concentrations of 37 bp DNA. All experiments were performed at least in triplicate.

EMSA with 4WJ (4WJ) DNA was performed as described, using the following oligonucleotides (*29*):

(1) 5′-CCCTATAACCCCTGCATTGAATTCCAGTCTGATAA-3′

(2) 5′-GTAGTCGTGATAGGTGCAGGGGTTATAGGG-3′

(3) 5′-AACAGTAGCTCTTATTCGAGCTCGCGCCCTATCACGACTA-3′

(4) 5′-TTTATCAGACTGGAATTCAAGCGCGAGCTCGAATAAGAGCTACTGT-3′.

The 4WJs were prepared by annealing of strands 1−4, followed by purification of the junctions on native polyacrylamide gels. The integrity of the 4WJs was verified by separation of aliquots of gel purified junctions (subsequently ^{32}P-labeled at the 5′ termini) on a denaturing gel.

Ten femtomoles of DNA was incubated with 9 μL of cell lysate or 80 nM DrHU for 5 min and reactions loaded onto a prerun 10% acrylamide gel. The gel was run at 200 V for 3 h, dried, visualized by phosphorimaging and quantitated using ImageQuant 5.0. Cell lysates were incubated with DNA and increasing amounts of DrHU under the same conditions. Supershift assays were performed by assembling reactions containing cell lysate and/or DrHU as well as anti-histone H1 antibody.

Two-Dimensional Methidium Propyl EDTA (MPE)-Fe(II) Footprinting. Two-dimensional footprinting was performed essentially as described (*29*): protein−DNA complexes were formed in a 10 μL volume for 5 min at room temperature under reaction conditions as described above, except that each reaction contained 0.4 pmol of DNA. DNA cleavage was performed by addition of 1 μL of 10 mM sodium ascorbate (0.8 mM final concentration) and 2 μL of freshly prepared 25 μM MPE-Fe(II) (final concentration 3.8 μM) for two minutes, and reactions were terminated by loading on a 8% native polyacrylamide gel. Protein−DNA complexes were isolated, and the DNA was passively eluted from gel slices, extracted with phenol-chloroform, precipitated with ethanol, and resolved on a 15% denaturing gel. Density profiles were obtained by phosphorimaging.

Supercoiling Assays. Negatively supercoiled pGEM5 (100 ng/reaction) was relaxed with Vaccinia topoisomerase I (Epicentre), and reactions performed as previously described (*29*). Briefly, relaxed DNA was incubated with topoisomerase and increasing amounts of HU at 37 °C for 60 min and reactions terminated by addition of 5 μL termination mix (5× TBE, 5% SDS, 15% sucrose, 0.1% bromophenol blue, 0.1% xylene cyanol, 2 μg/μL proteinase K), followed by a further incubation for 60 min. Reactions were resolved on a 1% agarose gel run at 25 V for 14 h, and DNA topoisomers were visualized by ethidium bromide staining following electrophoresis.

DNA Cyclization Assay. DNA (105 bp) was prepared by restriction digestion of pET5a as described (*29*). Time course ligation experiments with increasing (HU) were carried out as follows: reactions containing 100 fmol of DNA and the desired concentration of HU were incubated in 1× binding buffer with 1× ligase buffer (New England Biolabs) and 0.5 mM ATP in the presence of 80 U of T4 DNA ligase at room temperature for the desired time. Reactions were terminated with 75 mM EDTA, 3 mg/mL proteinase K, 15% glycerol, and bromophenol blue and xylene cyanol, followed by 15 min incubation at 55 °C, analyzed on 8% native polyacrylamide gels and quantitated by phosphorimaging.

RESULTS

N-Terminally Truncated DrHU Is Folded in Solution. While almost all HU proteins consist of the 90−99 amino acid type II DNA binding fold, DrHU has an additional 47-amino acid N-terminal domain preceding this DNA-binding motif (Figure 1). The sequence of the N-terminal extension is rich in lysine and highly repetitive, containing three APA-(A/K)K repeats, and its similarity to the C-terminus of eukaryotic histone H1 with its (S/T)PKK repeats (*36*, *37*), predicts its participation in DNA interactions. To specify the function of the DrHU N-terminal domain, a truncated protein, ΔDrHU, was prepared in which the 47 N-terminal amino acids are deleted. ΔDrHU was purified to ∼95% homogeneity (Figure 2).

While full-length DrHU primarily exists as a dimer in solution, with higher order aggregates predominating at higher protein concentrations (Figure 2 and (*29*)), cross-

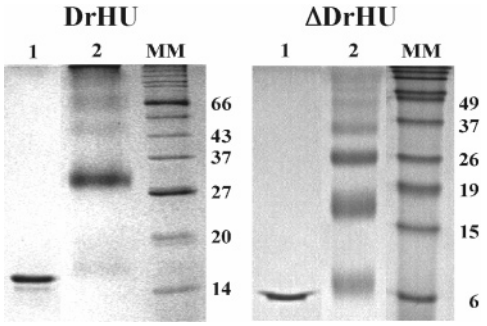

FIGURE 2: ΔDrHU forms oligomeric assemblies in solution. Lanes 1 contains 1 μg of unmodified protein; lanes 2 contain 7 μg of DrHU (right panel) or ΔDrHU (left panel) cross-linked with glutaraldehyde. Molecular mass markers, indicated at the right, are in kDa. DrHU and ΔDrHU were analyzed on 17 and 20% SDS−PAGE gels, respectively.

linking of ΔDrHU with 0.1% glutaraldehyde shows that it exists both as a dimer as well as other multimeric assemblies, as seen also for other HU homologues (*29*, *31*, *38*). For full-length DrHU (*29*), we have previously shown that cross-linked product corresponding to a dimer is the predominant species, regardless of protein concentration, suggesting that it corresponds to a stable dimer as opposed to a collisional intermediate, the appearance of which would be expected to increase with increasing protein concentrations. Likewise, dimeric ΔDrHU is the most abundant species, even at lower protein concentrations (data not shown). The formation of cross-linked species is attenuated upon cross-linking of ΔDrHU at 0 °C, but incubation at 0 °C has no effect on cross-linking of the full-length protein (data not shown). The far UV CD-spectrum of ΔDrHU shows that the truncated protein is folded, and that its secondary structure content is comparable to that of other HU homologues (Figure 3A; *39*−*41*).

A glycine in the loop connecting helices I and II has been suggested to correlate with thermostability of HU from thermophilic organisms (*40*−*43*). *Deinococcaceae* are most closely related to the thermophilic genus *Thermus*, and DrHU conserves this glycine (Figure 1). However, denaturation of ΔDrHU yields a melting temperature of 46.4 ± 0.1 °C (Figure 3B), similar to that of HU from mesophilic organisms (*40*). We also note the marked increase in ellipticity at ∼220 nm on reducing the temperature from ∼30 °C to 5 °C, indicating conformational changes associated with lower temperatures. This is consistent with the reduced cross-linking efficiency of ΔDrHU at 0 °C and suggests an inability of unfolded or improperly folded protein to dimerize.

Binding Site Size of ΔDrHU. While full-length DrHU is unable to form complex with 37 bp duplex DNA that is stable to electrophoresis (Figure 4B), ΔDrHU forms multiple complexes. An estimate of the active fraction of ΔDrHU was made by titrating 0.5 μM ΔDrHU with increasing concentrations of 37 bp duplex DNA, yielding saturation of the protein at ∼150 nM DNA, corresponding to 90% activity of the protein preparation, assuming association of three protein dimers per DNA molecule, as suggested by the formation of three distinct complexes (data not shown). We note that this estimate is consistent with the fraction of ΔDrHU that fails to cross-link with glutaraldehyde (Figure 2).

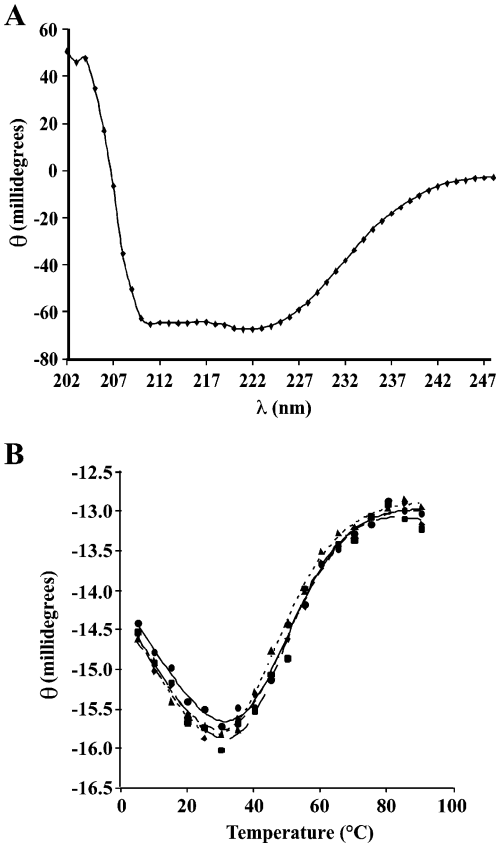

FIGURE 3: Circular dichroism spectroscopy of ΔDrHU. (A) Far UV CD spectrum of ΔDrHU reflecting significant α-helical content. (B) Melting curve of ΔDrHU. Thermal denaturation was recorded from 5° to 90° for wavelengths 218 (●), 219 (■), 220 (◆) and 221 (▲) nm. The reduced magnitude of the ellipticity compared to panel (A) is due to lower protein concentration.

Quantitation of complex formation with 37 bp DNA shows no indication of cooperativity; fits of the data to the Hill equation yields a Hill coefficient of 1.0 ± 0.1 and a half-maximal saturation of 19.9 ± 1.6 nM. To calculate the occluded site size, a 50 bp duplex DNA was generated by extension of either end of the 37 bp duplex. Under stoichiometric conditions, where (DNA) > K_d (Figure 5B−C), a break is seen at the equivalence point, where the molar ratio of lattice residues (base pairs) to ligand concentration is equal to site size, and a DNA site size for ΔDrHU of 11 ± 1 bp was measured. As the total length of the DNA is relatively short compared to the calculated site size, apparent negative cooperativity is seen as it becomes increasingly difficult to saturate the DNA probe (a statistical effect, not necessarily reflecting modification of adjacent binding sites), leading to an underestimate of the protein concentrations required to saturate the DNA and an overestimate of the site size. Notably, the number of complexes seen on 37 bp DNA is comparable to the three complexes formed by *E. coli* HU on 29 bp DNA, which led to the inference of a 9 bp site size (*32*). Half-maximal saturation of 6.2 ± 0.6 nM is seen for 50 bp DNA (Figure 5D). Thus, removal of the N-terminal domain allows the truncated protein to engage duplex DNA with a binding site size comparable to the ∼9 bp site reported for *E. coli* HU (*10*, *32*). The reduced DNA site size of ΔDrHU suggests that the N-terminal domain prevents the interaction with short duplex DNA seen for other HU homologues. In contrast, extension of the duplex to 50 bp

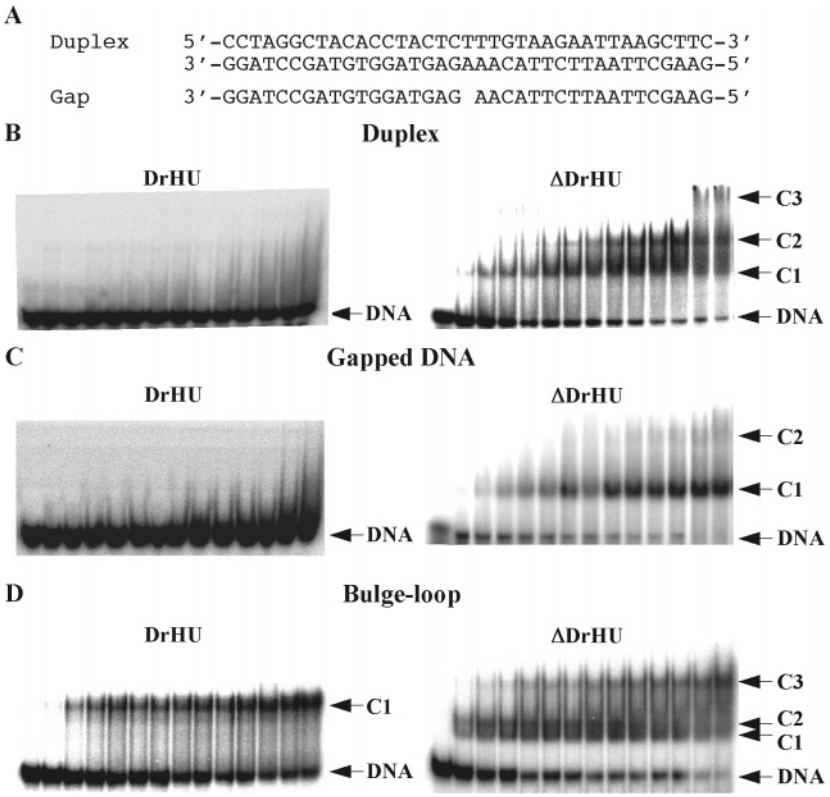

FIGURE 4: ΔDrHU binds preferentially to distorted DNA. (A) Sequence of 37 bp duplex and duplex with 1-nt gap. To generate nicked DNA, an extra adenosine was included at the 3′-end of the first bottom strand. Bulged DNA was generated by inserting three unpaired cytosines at the center of the bottom strand, as illustrated previously (*29*). (B−D) Electrophoretic analysis of DrHU (left panels) and ΔDrHU (right panels) with (B) 37 bp duplex DNA; (C) 1 nt-gap DNA; (D) DNA with bulge-loops. Complexes (C1−C3) are indicated at the right. [DrHU] are 25−600 nM and [ΔDrHU] are 0−1.0 μM for panels (B−C); for panel (D) 0−100 nM.

yields a single stable complex with full-length DrHU, indicating a contribution of the N-terminus to DNA binding (Figure 5A; *29*).

Architectural Properties of ΔDrHU. Full-length DrHU has little preference for flexible DNA structures such as DNA with nicks, gaps, or mismatches; for example, no stable complex may be detected on 37 bp duplex with a central gap (Figure 4C), and we have previously shown that complex formation of DrHU with 89 bp duplex DNA or 89 bp DNA containing a central nick is comparable, both in terms of number of complexes and half-maximal saturation (*29*). In contrast, electrophoretic mobility shift assays (EMSAs) with ΔDrHU show that it preferentially forms a single complex with 37 bp duplex DNA with 4-nt loops or a central nick or gap, while multiple complexes are seen with perfect duplex DNA (Figure 4A−C and data not shown). As structural and biochemical analyses of HU proteins have shown that placement of nicks, gaps, or mismatches at the site of the proline intercalation often results in preferred binding to the more flexible DNA substrate, our data suggest that ΔDrHU engages the 37 bp DNA in an equivalent manner, as expected, but that the N-terminal domain prevents recognition of the flexure points. Like full-length DrHU, ΔDrHU exhibits no preference for 37 bp duplex DNA with a G+C-content of 67%, comparable to the G+C-content of *D.* radiodurans genomic DNA, compared to DNA with average G+C-content (data not shown). DNA in which two bulge-loops of three C's were introduced at a distance of 9 bp (*29*) binds ΔDrHU with only modestly increased preference compared to perfect duplex DNA, forming multiple complexes with a half-maximal saturation of 8.2 ± 1.3 nM (Figure 4D). By comparison, full-length DrHU forms a single complex on 37 bp DNA with bulge-loops with K_d = 128 nM (Figure 4D; *29*).

Full-length DrHU has a modest ability to introduce negative supercoils into relaxed DNA in the presence of topoisomerase (*29*). However, ΔDrHU is unable to constrain DNA supercoils (Figure 6). Evidently, the ability of DrHU to wrap DNA into negative toroidal supercoils is abolished with removal of the N-terminus, consistent with a contribution of this domain to DNA binding. To assess DNA bending by ΔDrHU, a cyclization assay was used in which DNA shorter than the persistence length is cyclized with T4 DNA ligase. Like wild-type DrHU (*29*), ΔDrHU is unable to promote cyclization of 105 bp DNA or 105 bp duplex DNA with a central nick, suggesting its inability to induce a significant DNA bend (data not shown) and suggesting that the failure of full-length DrHU to promote DNA cyclization is not merely a consequence of the presence of the N-terminal extension.

DrHU and ΔDrHU Interact Differently with Four-Way Junction DNA. A 4WJ DNA was generated as reported for analysis of *E. coli* HU and full-length DrHU (*10*, *29*). While full-length DrHU forms two distinct complexes with this DNA with half-maximal saturation of 18 nM (Figure 7A; *29*), ΔDrHU forms multiple complexes under identical conditions (Figure 7B), consistent with a different stoichiometry of binding, with half-maximal saturation 1.4 ± 0.4 nM (Figure 7C). Linear duplex DNA corresponding to the two arms of the 4WJ, a 35-mer and a 40-mer respectively,

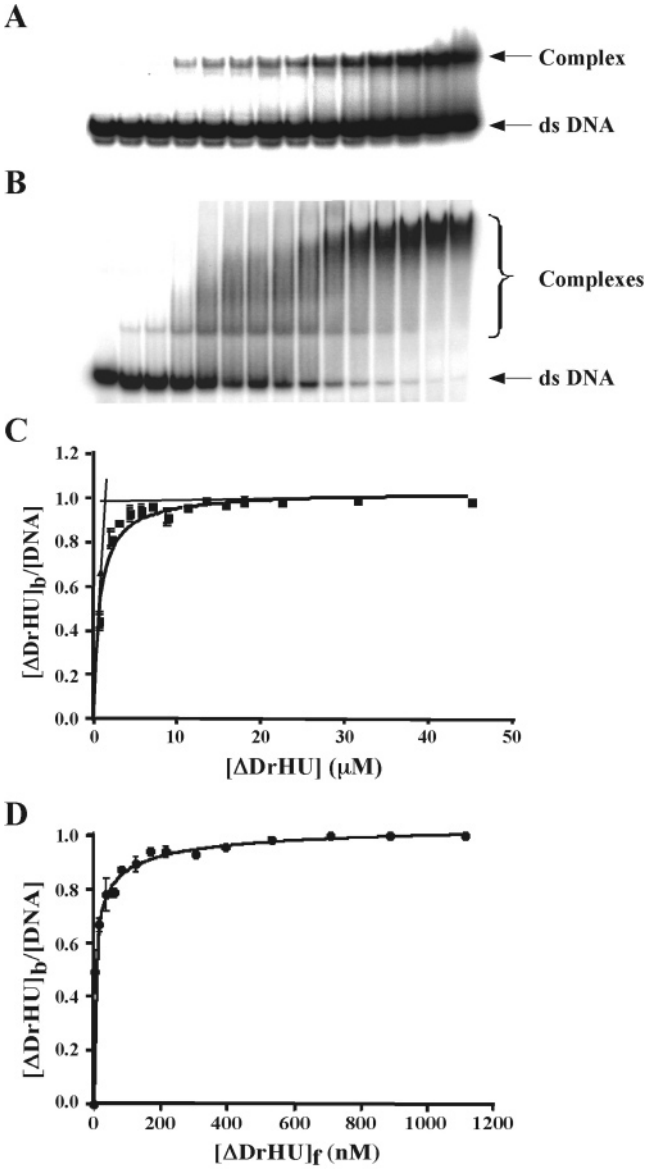

FIGURE 5: Interaction with 50 bp DNA. (A) DrHU forms a single complex; [DrHU] are 10−600 nM. (B) Electrophoretic analysis of 50 bp duplex DNA titrated with ΔDrHU under stoichiometric conditions. Complexes are indicated at the right. Each reaction contained 0.5 μM DNA and 0−50 μM protein. (C) Ratio of bound ΔDrHU to total 50 bp DNA as a function of [ΔDrHU]. The concentration of ΔDrHU corresponding to the intercept of tangents to the initial slope and the final plateau reflects the stoichiometry of the interaction, yielding a site size of ~11 bp. (D) Binding isotherm for 10 nM 50 bp DNA titrated with ΔDrHU; fits of the data to the Hill equation yield $f_{max} = 1.06$, reflecting complex stability during electrophoresis.

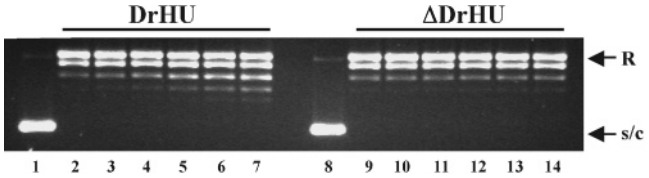

FIGURE 6: ΔDrHU does not supercoil DNA. Supercoiling of relaxed DNA (R) in the presence of topoisomerase I and 0, 0.1, 0.25, 0.5, 0.75, 1.0 μM of DrHU (lanes 2−7) and ΔDrHU (lanes 9−14). Lanes 1 and 8, supercoiled (s/c) pGEM5 DNA.

showed the same binding pattern as seen with 37 bp duplex DNA (data not shown). This is consistent with a shorter site size for ΔDrHU but retention of preferred binding to the bent DNA structure.

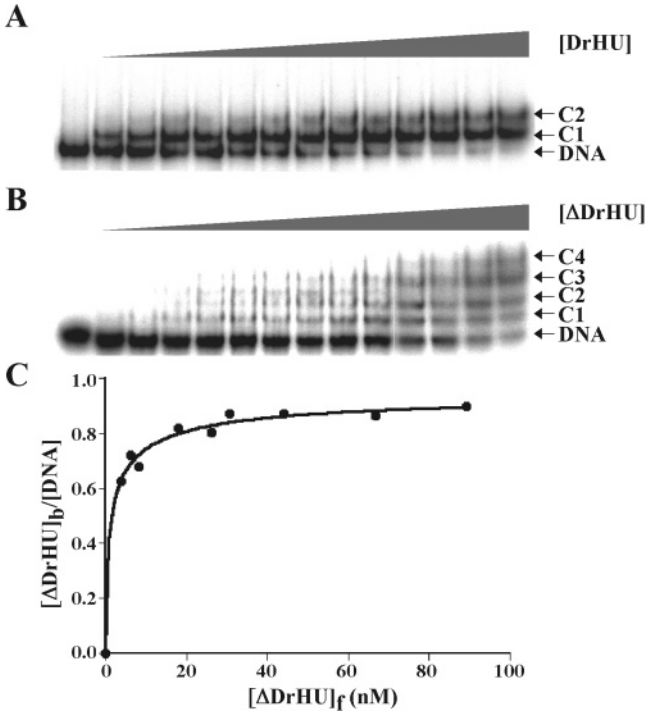

FIGURE 7: ΔDrHU forms multiple complexes with four-way junction DNA. (A) Two distinct complexes are formed with DrHU (0−80 nM). Complexes (C1, C2) are indicated at the right. (B) Electrophoretic analysis of ΔDrHU with increasing concentrations of ΔDrHU (0−100 nM). Each reaction contained 1.0 nM DNA. Complexes (C1−C4) and free DNA are indicated at the right. (C) Binding isotherm for ΔDrHU binding to 4WJ DNA; fits of the data to the Hill equation yield $f_{max} = 0.96$, reflecting the absence of significant complex dissociation during electrophoresis.

The position of ΔDrHU on the 4WJ was assessed by two-dimensional MPE-Fe(II) footprinting, measuring ΔDrHU binding to the stacked X junction conformation preferred in the presence of Mg^{2+} (Figure 8A−D) (*44*−*46*). We separately assayed binding of ΔDrHU in complexes 1 and 2, the two complexes of highest mobility, to compare with the full-length protein. For full-length DrHU, complex 1 shows protein protecting only the 3′-ends of strands 2 and 3, while complex 2 also reveals protection toward the 3′-ends of strands 1 and 4, in both cases coupled with enhanced cleavage at the crossover of the opposite strands (Figure 8E). This pattern of cleavage indicates preferred binding of DrHU to one pair of junction arms, resulting in the predominance of one of the two possible conformational isomers of the junction (*29*). The pattern of protection by ΔDrHU is significantly different: Comparison of densitometric traces shows little difference between the cleavage patterns in complex 1 and 2, immediately indicating that the preferred binding to a specific pair of junction arms seen for full-length DrHU is lost on removal of the N-terminus (Figure 8A−D). For both complex 1 and complex 2, partial protection of strands 2 and 3 is evident, both upstream and downstream of the crossover. Notably, no protection is evident distal to the crossover, as seen for full-length DrHU (compare Figure 8, panels E and F). For strands 1 and 4, the appearance of modestly enhanced cleavage coincides with reduced signal attributable to the loss of short cleavage products during native gel electrophoresis, and it therefore most likely

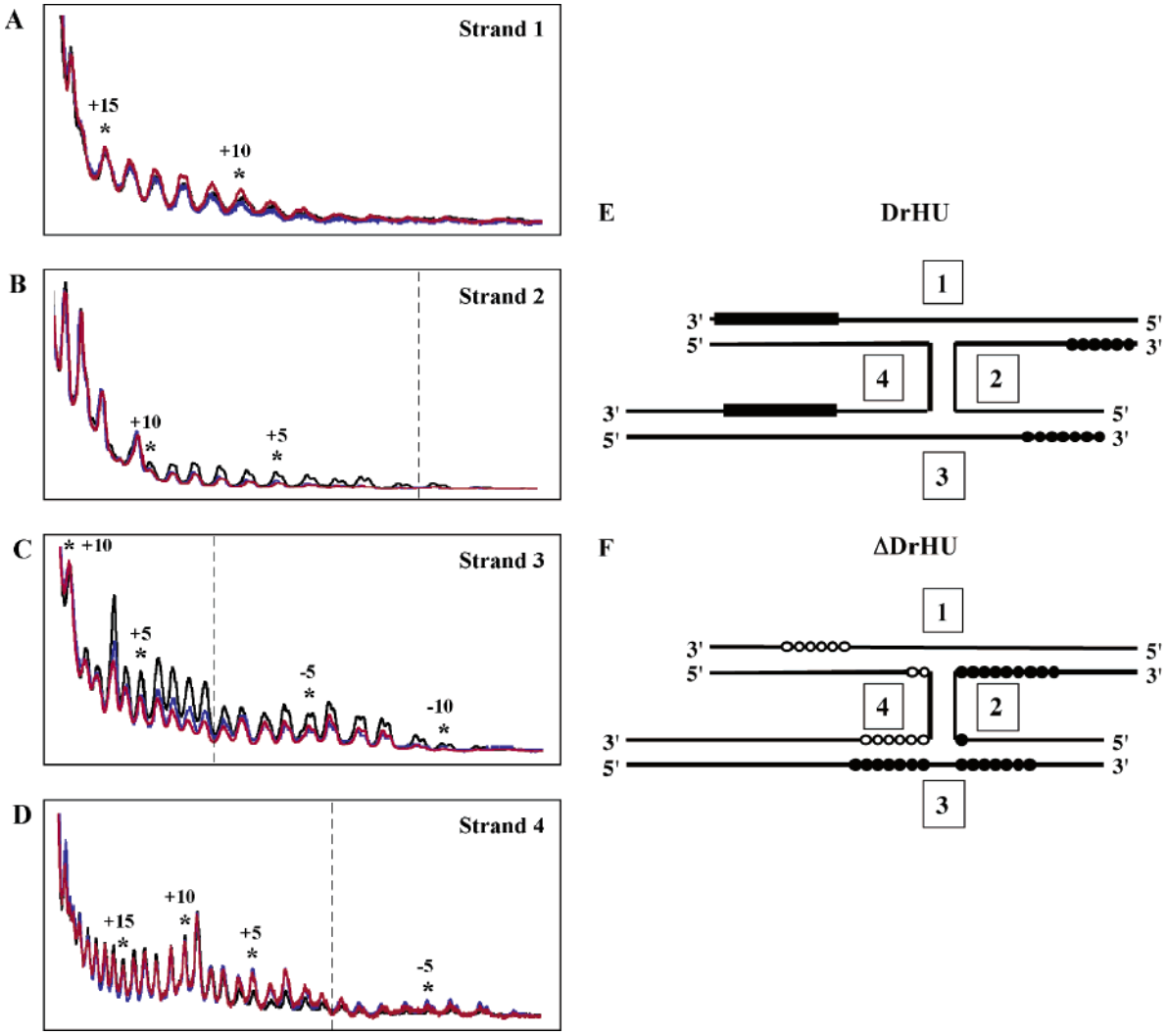

FIGURE 8: DrHU and ΔDrHU interact differently with 4WJ DNA. (A−D) Densitometric profiles corresponding to ΔDrHU complex 1 (blue) and complex 2 (red) on strands 1−4, respectively. Free DNA is in black. The vertical dotted line identifies the crossover, with positive and negative numbers identifying positions downstream and upstream of the crossover, respectively. (E) Summary of cleavage pattern for full-length DrHU with (●) and (■) representing protection in complex 1 and 2, respectively. Adapted from (*29*). (F) Summary of cleavage pattern for ΔDrHU with (●) representing protection and (○) representing retention of smaller cleavage products in complex 1 and 2. Only one conformational isomer of the stacked X junction conformation is indicated, corresponding to that preferred by full-length DrHU, although data for ΔDrHU indicate no preference for either conformer.

corresponds to bound protein preventing this loss. These patterns of partial protection suggest that ΔDrHU interacts with all four strands of the junction close to the crossover, as previously reported for *E. coli* HU, but in distinct contrast to full-length DrHU which protects the junction only distal to the crossover (*10*, *12*, *29*).

DrHU May Serve To Stabilize Four-Way Junction DNA in Vivo. The N-terminal domain of DrHU bears significant sequence similarity to the (S/T)PKK motifs found in the C-terminal domain of histone H1; DrHU contains three APA-(A/K)K repeats (Figure 1). Indeed, probing DrHU and ΔDrHU with antibodies against histone H1 by Western blotting shows that DrHU is recognized by antibodies to histone H1, whereas ΔDrHU is not (Figure 9A,B), suggesting that the lysine-containing repeats in DrHU mimic those of histone H1.

The only protein from *D. radiodurans* cell lysate that is recognized by the anti-H1 antibody migrates equidistant with the purified DrHU (Figure 9B). We therefore explored the possibility that DrHU might be present in sufficient quantity in *D. radiodurans* lysates to be detected via its preferred binding to 4WJ DNA. Pull-down assays using biotin-conjugated 4WJ DNA immobilized on streptavidin-beads proved unsuccessful, as DrHU was found to bind avidly to streptavidin (not shown). Binding of *D. radiodurans*-encoded proteins to 4WJ was therefore assessed using EMSA. However, upon incubation of the cell lysate with the 4WJ DNA, a complex was formed which migrated much slower than the DrHU−DNA complex (Figure 9C, compare lanes 3 and 5). Addition of increasing amounts of recombinant DrHU to the cell lysate−DNA mixture resulted in enhanced formation of the slow-migrating complex only (Figure 9C, lanes 5−9), suggesting that this complex contains DrHU as well as other protein(s) that recognize the 4WJ. The complex formed with 4WJ DNA in the presence of DrHU or cell lysate, respectively, was completely disrupted in the presence of the antibody, which indicates its interaction with a protein in the complex (Figure 9C, lanes 4 and 10). Since Western blotting identified only one protein from *D. radiodurans* lysates with reactivity toward the anti-H1 antibody and since

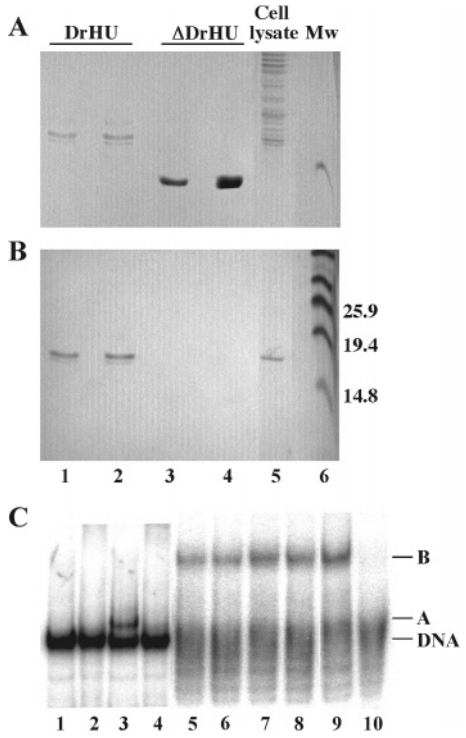

FIGURE 9: Four-way junction DNA assembles a complex containing DrHU. (A) SDS−PAGE gel with increasing concentrations of DrHU (lanes 1−2), ΔDrHU (lanes 3−4) and *D. radiodurans* cell lysate (lane 5). Prestained molecular weight marker is in lane 9. Gel was stained with Coomassie after transfer. (B) Western blotting of gel shown in (A) using antibody against histone H1. (C) EMSA showing incubation of 4WJ DNA with DrHU, with DrHU-DNA complex identified as complex A, and coincubation of cell lysate with increasing amounts of DrHU as complex B. Lane 1, DNA only; lane 2, DNA with antibody; lane 3, DNA with DrHU (0.8 pmol); lane 4, DNA with DrHU (0.8 pmol) and antibody; lane 5, DNA with cell lysate (9 μl); lanes 6−9, DNA with cell lysate and increasing amounts of DrHU up to 25 pmol; lane 10, DNA with cell lysate, DrHU (25 pmol) and antibody. The DNA degradation observed in lanes 5−10 is due to the presence of nucleases in the cell lysate.

this protein comigrates with purified DrHU, this is consistent with 4WJ DNA associating with DrHU as well as other *D. radiodurans*-encoded protein(s). These observations show that the extended form of DrHU is present in vivo and support our suggestion that DrHU is involved in stabilization of 4WJ structures in vivo and that the role of the N-terminal domain is to confer unique placement of DrHU on 4WJ DNA.

DISCUSSION

Sequence and Structural Considerations. On the basis of the sequence similarity of the DrHU N-terminal domain to that of the histone H1 C-terminus, we predicted its interaction with DNA. However, the N-terminus appears not only to contact DNA, as evidenced by the failure of ΔDrHU to constrain DNA supercoils and by the ability of the N-terminal domain to mediate a distinct mode of binding to 4WJ DNA (Figures 6−8), but also to attenuate the interaction of the core domain with DNA, as shown by the ability of DrHU to bind stably only to DNA longer than ∼50 bp, while ΔDrHU binds much shorter duplexes (Figures 4 and 5). Notably, ΔDrHU also retains a modest ability to distinguish between perfect duplex and duplex with flexure points such as nicks and gaps, while full-length DrHU has lost this ability. While both full-length and truncated proteins bind preferentially to 4WJ DNA, their placement on the junction differs significantly (Figure 8). Accordingly, the function of the DrHU N-terminal domain appears to be two-fold: to attenuate affinity for DNA with flexure points and to direct DrHU to a distinct mode of interaction with 4WJ DNA.

Comparison of the sequence of DrHU with that of other HU homologues reveals significant conservation of the type II DNA-binding fold, suggesting its existence as a dimer (as confirmed by cross-linking, Figure 2) and its interaction with DNA through intercalation of conserved proline residues (Figure 1). DrHU has a glycine in the loop between helices 1 and 2, otherwise found in HU from thermophiles, where its presence has been associated with loop flexibility and increased thermal stability. However, ΔDrHU shows no such enhanced stability. In *B. stearothermophilus* HU, substitution of Gly with Glu leads to a reduction in Tm from 64 to 54 °C, while the reciprocal mutation of Glu to Gly in *B. subtilis* HU (HBsu) increases loop flexibility, and in the *B. subtilis* bacteriophage SPO1-encoded HU homolog, TF1, it increases the T_m by 11 °C (*38*, *40*−*43*). On the basis of the T_m reported for HBsu of 48.6 °C measured by CD spectroscopy in phosphate buffer pH 7.0 with 200 mM NaCl (*40*), the T_m of 46.4 °C measured for ΔDrHU under somewhat less stringent conditions (Figure 3) reflects comparable thermal stability. Whether absence of the N-terminal tail affects thermal stability or the cold-sensitive behavior of ΔDrHU awaits precise determination.

The secondary structure of ΔDrHU based on the far-UV CD spectrum shows a conformation similar to that of other HU homologues. These observations suggest that the N-terminus is not required for folding of ΔDrHU and that it may constitute a separate domain of DrHU. The N-terminal tail of *D. radiodurans* HU contains three APA(A/K)K repeats, reminiscent of the (S/T)PKK repeats found in the C-terminus of eukaryotic histone H1. This C-terminal tail is disordered in aqueous solution but becomes ordered on DNA binding or in trifluoroethanol (*37*, *47*). The similarity of the repeat sequences predicts that the N-terminus of uncomplexed DrHU may also be unfolded due to charge repulsion.

Substrate Selectivity of ΔDrHU. ΔDrHU has a nonspecific DNA site size of ∼11 bp, comparable to the site size reported for *E. coli* HU (*32*). ΔDrHU also retains the ability to distinguish between duplex DNA and DNA with nicks or gaps (Figure 4). These observations suggest that ΔDrHU engages DNA as seen, for example, in the *Anabaena* HU−DNA cocrystal structure in which two DNA kinks are produced by intercalating prolines, while the intervening 9 bp of duplex contact the positively charged "saddle" formed by intertwining β-strands (Figure 10). The lack of supercoiling by ΔDrHU suggests that it must be either unable to wrap DNA or that the path of wrapping is not consistent with the constraint of supercoils (for example, the HU homologue IHF wraps DNA that lies in nearly a single plane, with the wrapped DNA attaining only a small dihedral angle of ∼10−15° (*7*), while *Anabaena* HU introduces a larger dihedral angle that leads to DNA supercoiling (*8*)).

Surprisingly, full-length DrHU has lost the ability to engage short DNA duplexes stably, and the ability to distinguish duplex DNA from DNA with nicks or gaps is also absent (Figure 4). If the N-terminal segments merely

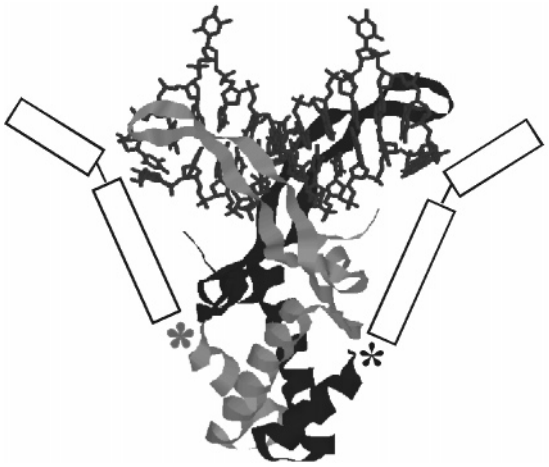

FIGURE 10: Model of *Anabaena* HU with 11 bp DNA (pdb 1P71) showing interaction between the positively charged β-strands and the 9 bp of duplex flanked by proline-mediated DNA kinks. Protein is shown in ribbon representation with different shading for each monomer. Proposed locations of N-terminal segments are indicated as open rectangles with asterisks marking the N-termini of the conserved type II DNA binding fold. Model generated with RasMol.

extended the region of DNA contact, then the expectation would be for interaction with short duplexes and preferred binding to nicked or gapped DNA to be retained, and for DrHU simply to exhibit greater affinity for longer duplexes. However, we find that DrHU has lost the binding properties characteristic of ΔDrHU, suggesting that the N-terminal segments prevent the interaction between DNA and the HU core domain, perhaps through interaction between the N-terminal segments and the protruding β-arms, and that only DNA that is long enough to engage both N-terminal segments of the dimer permits stable complex formation (Figure 10).

DrHU has been shown to interact stably only with duplex DNA of ~50 bp or longer (*29*). The longest site size for HU homologues is featured in the structure of *E. coli* IHF with DNA in which 35 bp of DNA is seen to wrap the entire body of the protein, resulting in an ~140 degree DNA bend (*7*). Contacts to DNA longer than ~11 bp would demand DNA bending (e.g., as seen in the cocrystal structure of IHF or *Anabaena* HU with DNA) as the DNA changes direction from laying across the beta-sheet structure at the top of the HU dimer to wrapping along the lateral sides of the body (*48*). In other words, the dimensions of the compact dimer precludes interaction with longer DNA without introduction of a significant DNA bend. For the N-terminal extensions to modulate the structure in such a way as to allow interactions across a long DNA duplex, without themselves interacting with the DNA, is difficult to imagine, given the conservation and compactness of the HU fold. Importantly, no DNA bending of linear DNA by DrHU can be detected, as determined by cyclization of duplex DNA of varying length (*29*). While our data clearly implicate the N-terminal extensions in obscuring interaction with the conserved type II DNA binding fold characteristic of the protein core, defining the precise mode of contact with the N-termini awaits further documentation.

Both DrHU and ΔDrHU have higher affinity for 4WJ structures. In the stacked X conformation, the 4WJs are expected to exist as an equilibrium mixture of two conformational isomers, pairing different sets of junction arms (*44*−*46*). When full-length DrHU binds to 4WJ DNA, initial binding involves only one pair of junction arms, with the pattern of cleavage suggesting that DrHU is positioned between the junction arms, protecting interior strands, leaving the crossover region of the other two strands exposed (*29*). At higher protein concentrations, a second complex forms in which the opposite pair of junction arms is also protected (*29*). However, with removal of the N-terminal domain, multiple complexes form, immediately suggesting an altered mode of interaction with the 4WJ DNA (Figure 7B). Densitometric profiles from two-dimensional MPE-Fe(II) footprinting show that the patterns of cleavage in complex 1 and 2, the two complexes of highest mobility, are qualitatively similar (Figure 8A−D), signifying that ΔDrHU exhibits no preferred binding to a specific pair of junction arms. Yet, the presence of protected segments reflects preferred and not random binding to the junction. Protection is seen on either side of the crossover for strands 3 and 2, although strand 2 is too short to specify interactions 5′ to the crossover. For strands 1 and 4, interactions at the crossover are suggested by the greater retention of small cleavage products. Accordingly, our data indicate that ΔDrHU contacts all four strands near the crossover, with little or no preference for either side of the junction or for either junction conformer.

For *E. coli* HU binding to 4WJ DNA, a series of complexes were seen, resembling the pattern of complexes formed with ΔDrHU. These complexes were interpreted to represent stoichiometric isomers, as additional retarded complexes were seen at higher protein concentrations, with the concomitant disappearance of complexes of higher electrophoretic mobility (*12*). However, we cannot rule out the possibility that the additional complexes may represent conformational isomers; even though the 4WJ is expected to adopt the stacked X conformation under the experimental conditions used, it is conceivable that alternate structures may form upon protein binding. Whether the additional complexes represent stoichiometric or conformational isomers, the mode of interaction is clearly different from that exhibited by full-length DrHU.

For *E. coli* HU, binding to 4WJ DNA was proposed to involve interaction of one β-arm with the crossover, while the other β-arm of the HU dimer would contact duplex DNA 3′ to the crossover, unable to introduce a DNA kink (*12*). ΔDrHU may engage the junction similarly, except that the protection of strand 3 on either side of the junction suggests that the second β-arm may contact duplex DNA either 3′ or 5′ to the crossover. This distinction may be due to ΔDrHU being homodimeric, while *E. coli* HU is a heterodimer, leading to asymmetric binding. Taken together, our data show that the N-terminal domain of DrHU confers a unique placement of the protein on 4WJ DNA that leaves the crossover exposed, consistent with a paucity of interaction with the HU core domain, and consistent with an inability of a "bulkier" DrHU dimer to fit the geometry of the junction crossover. We suggest that DrHU serves to stabilize 4WJ structures, perhaps to allow access of other protein(s) involved in DNA recombination. This interpretation is supported by our EMSA analysis using *D. radiodurans* lysates which suggest that DrHU interacts with other protein(s) in the presence of the 4WJ DNA (Figure 9).

The remarkable resistance of *D. radiodurans* to extreme doses of ionizing radiation and prolonged periods of desic-

cation may be a result of accurate and extensive template-independent DNA recombination events facilitated by restricted diffusion of DNA fragments, as well as template-dependent recombination (*26*). As DrHU is expected to be present at significant concentrations (μM) in the cell, and since it binds with high affinity to 4WJ DNA, it may recognize these recombination intermediates, and direct other recombination-specific proteins to the crossover region (*28*, *49*, *50*). As a functional RecA protein is required for bringing together overlapping DNA fragments in *D. radiodurans* resistance phenotypes, other recombination proteins, including RecQ helicase or the junction resolving enzymes RuvA, B, or C may be speculated to interact with DrHU as it stabilizes 4WJ structures in preparation for subsequent repair events (*27*, *28*, *51*, *52*).

ACKNOWLEDGMENT

We thank P. DiMario for suggesting the use of antibody to histone H1 and for providing it, and J. Battista for helpful comments.

REFERENCES

1. Drlica, K., and Rouvière-Yaniv, J. (1987) Histonelike proteins of bacteria, *Microbiol. Rev. 51*, 301−319.
2. Kellenberger, E., and Arnold-Schultz-Gahmen, B. (1992) Chromatins of low-protein-content: special features of their compaction and condensation, *FEMS Microbiol. Lett. 100*, 361−370.
3. Azam, T. A., and Ishihama, A. (1999) Twelve species of the nucleoid-associated protein from *Escherichia coli* sequence recognition specificity and DNA binding affinity, *J. Biol. Chem. 274*, 33105−33313.
4. Tanaka, I., Appelt, K., Dijk, J., White, S., and Wilson, K. (1984) 3-Å resolution structure of a protein with histone-like properties in prokaryotes, *Nature 310*, 376−381.
5. White, S. W., Appelt, K., Wilson, K. S., and Tanaka, I. (1989) A protein structural motif that bends DNA, *Proteins: Struct. Funct. Genet. 5*, 281−288.
6. Vis, H., Mariani, M., Vorgias, C. E., Wilson, K. S., Kaptein, R., and Boelens, R. (1995) Solution structure of the HU protein from *Bacillus stearothermophilus*, *J. Mol. Biol. 254*, 692−703.
7. Rice, P. A., Yang, S. W., Mizuuchi, K., and Nash, H. A. (1996) Crystal structure of an IHF-DNA complex: a protein-induced DNA U-turn, *Cell 87*, 1295−1306.
8. Swinger, K. K., Lemberg, K. M., Zhang, Y., and Rice, P. A. (2003) Flexible DNA bending in HU-DNA cocrystal structures, *EMBO J. 22*, 3749−3760.
9. Pontiggia, A., Negri, A., Beltrame, M., and Bianchi, M. E. (1993) Protein HU binds specifically to kinked DNA, *Mol. Microbiol. 7*, 343−350.
10. Bonnefoy, E., Takahashi, M., and Rouvière-Yaniv, J. (1994) DNA-binding parameters of the HU protein of *Escherichia coli* to cruciform DNA, *J. Mol. Biol. 242*, 116−129.
11. Castaing, B., Zelwer, C., Laval, J., and Boiteux, S. (1995) HU protein of *Escherichia coli* binds specifically to DNA that contains single-strand breaks or gaps, *J. Biol. Chem. 270*, 10291−10296.
12. Kamashev, D., Balandina, A., and Rouvière-Yaniv, J. (1999) The binding motif recognized by HU on both nicked and cruciform DNA, *EMBO J. 18*, 5434−5444.
13. Kamashev, D., and Rouvière-Yaniv, J. (2000) The histone-like protein HU binds to DNA recombination and repair intermediates, *EMBO J. 19*, 6527−6535.
14. Rouvière-Yaniv, J., Yaniv, M., and Germond, J. E. (1979) *E. coli* DNA binding protein HU forms nucleosomelike structure with circular double-stranded DNA, *Cell 17*, 265−274.
15. Aki, T., and Adhya, S. (1997) Repressor induced site-specific binding of HU for transcriptional regulation, *EMBO J. 16*, 3666−3674.
16. Lavoie, B. D., and Chaconas, G. (1993) Site-specific HU binding in the Mu transposome: conversion of a sequence-independent DNA-binding protein into chemical nuclease, *Genes Dev. 7*, 2510−2519.
17. Bramhill, D., and Kornberg, A. (1988) A model for initiation at origins of DNA replication, *Cell 54*, 915−918.
18. Huisman, O., Faelen, M., Girard, D., Jaffe, A., Toussaint, A., and Rouvière-Yaniv, J. (1989) Multiple defects in *Escherichia coli* mutants lacking HU protein, *J. Bacteriol. 171*, 3704−3712.
19. Dri, A. M., Moreau, P. L., and Rouvière-Yaniv, J. (1992) Role of the histone-like proteins OmsZ and HU in homologous recombination, *Gene 120*, 11−16.
20. Boubrik, F., and Rouvière-Yaniv, J. (1995) Increased sensitivity to γ-irradiation in bacteria lacking protein HU, *Proc. Natl. Acad. Sci. U.S.A. 92*, 3958−3962.
21. Li, S., and Waters, R. (1998) *Escherichia coli* strains lacking HU are UV sensitive due to a role for HU in homologous recombination, *J. Bacteriol. 180*, 3750−3756.
22. Daly, M. J., and Minton, K. W. (1995) Interchromosomal recombination in the extremely radioresistant bacterium *Deinococcus radiodurans*, *J. Bacteriol. 177*, 5495−5505.
23. Mattimore, V., and Battista, J. R. (1996) Radioresistance of *Deinococcus radiodurans*: Functions necessary to survive ionizing radiation are also necessary to survive prolonged desiccation, *J. Bacteriol. 178*, 633−637.
24. Battista, J. R. (1997) Against all odds: the survival strategies of *Deinococcus radiodurans*, *Annu. Rev. Microbiol. 51*, 203−224.
25. White, O., Eisen, J. A., Heidelberg, J. F., Hickey, E. K., Peterson, J. D., Dodson, R. J., Haft, D. H., Gwinn, M. L., Nelson, W. C., and Richardson, D. L., et al. (1999) Genome sequence of the radioresistant bacterium *Deinococcus radiodurans* R1, *Science 286*, 1571−1577.
26. Levin-Zaidman, S., Englander, J., Shimoni, E., Sharma, A. K., Minton, K. W., and Minsky, A. (2003) Ringlike structure of the *Deinococcus radiodurans* genome: A key role to radioresistance, *Science 299*, 254−256.
27. Minton, K. W. (1996) Repair of ionizing-radiation damage in the radiation resistant bacterium *Deinococcus radiodurans*, *Mutat. Res. 363*, 1−7.
28. Kim, J.-I., and Cox, M. M. (2002) The RecA proteins of *Deinococcus radiodurans* and *Escherichia coli* promote DNA strand exchange via inverse pathways, *Proc. Natl. Acad. Sci. U.S.A. 99*, 7917−7921.
29. Ghosh, S., and Grove, A. (2004) Histone-like protein HU from *Deinococcus radiodurans* binds preferentially to four-way DNA junctions, *J. Mol. Biol. 337*, 561−571.
30. Grove, A., and Lim, L. (2001) High affinity DNA binding of HU protein from the hyperthermophile *Thermotoga maritima*, *J. Mol. Biol. 311*, 491−502.
31. Chen, C., Ghosh, S., and Grove, A. (2004) Substrate specificity of *Helicobacter pylori* is determined by insufficient stabilization of DNA flexure points, *Biochem J. 383*, 343−351.
32. Bonnefoy, E., and Rouvière-Yaniv, J. (1991) HU and IHF, two homologous histone-like proteins of *Escherichia coli*, form different protein-DNA complexes with short DNA fragments, *EMBO J. 10*, 687−696.
33. Grove, A., Galeone, A., Mayol, L., and Geiduschek, E. P. (1996) On the connection between inherent DNA flexure and preferred binding of hydroxymethyluracil-containing DNA by the type II DNA-binding protein TF1, *J. Mol. Biol. 206*, 196−206.
34. DiMario, P. J., and Gall, J. G. (1990) Nucleolin from the multiple nucleoli of amphibian oocyte nuclei, *Chromosoma 99*, 87−94.
35. Eftink, M. R., and Ramsay, G. D. (1994) Analysis of multidimensional spectroscopic data to monitor unfolding of proteins, *Methods Enzymol. 240*, 615−645.
36. Hendzel, M. J., Lever, M. A., Crawford, E., and Th'ng, J. P. H. (2004) The C-terminal domain is the primary determinant of histone H1 binding to chromatin in vivo, *J. Biol. Chem. 279*, 20028−20034.
37. Bharath, M. M. S., Ramesh, S., Chandra, N. R., and Rao, M. R. S. (2002) Identification of a 34 amino acid stretch within the C-terminus of histone H1 as the DNA-condensing domain by site-directed mutagenesis, *Biochemistry 41*, 7617−7627.
38. Christodoulou, E., and Vorgias, C. E. (2002) The thermostability of DNA-binding protein HU from mesophilic, thermophilic and extreme thermophilic bacteria, *Extremophiles 6*, 21−31.
39. Woody, R. W. (1995) Circular dichroism, *Methods Enzymol. 246*, 34−71.
40. Kawamura, S., Kakuta, Y., Tanaka, I., Hikichi, K., Kuhara, S., Yamasaki, N., and Kimura, M. (1996) Glycine-15 in the bend between two alpha-helices can explain the thermostability of DNA binding protein HU from *Bacillus stearothermophilus*, *Biochemistry 35*, 1195−1200.

41. Christodoulou, E., Rypniewski, W. R., and Vorgias, C. E. (2003) High-resolution X-ray structure of the DNA-binding protein HU from the hyper-thermophilic *Thermotoga maritima* and the determinants of its thermostability, *Extremophiles 7*, 111−122.
42. Andera, L., Spangler, C. J., Galeone, A., Mayol, L., and Geiduschek, E. P. (1994) Interrelations of secondary structure stability and DNA-binding affinity in the bacteriophage SPO1-encoded type II DNA-binding protein TF1, *J. Mol. Biol. 236*, 139−150.
43. Liu, W., Vu, H. M., Geiduschek, E. P., and Kearns, D. R. (2000) Solution structure of a mutant of transcription factor 1: implications for enhanced DNA binding, *J. Mol. Biol. 302*, 821−830.
44. Lilley, D. M., and Clegg, R. M. (1993) The structure of the four-way junction in DNA, *Annu. Rev. Biophys. Biomol. Struct. 22*, 299−328.
45. Duckett, D. R., Murchie, A. I., Diekmann, S., von Kitzing, E., Kemper, B., and Lilley, D. M. (1988) The structure of the Holliday junction, and its resolution, *Cell 55*, 79−89.
46. Hays, F. A., Vargason, J. M., and Ho, P. S. (2003) Effect of sequence on the conformation of DNA holliday junctions, *Biochemistry 42*, 9586−9597.
47. Xu, X., Cooper, L. G., DiMario, P. J., and Nelson, J. W. (1994) Helix formation in model peptides based on nucleolin TPAKK motifs, *Biopolymers 35*, 93−102.
48. Grove, A. (2003) Surface salt bridges modulate DNA wrapping by the type II DNA-binding protein TF1, *Biochemistry 42*, 8739−8747.
49. Ali Azam, T., Iwata, A., Nishimura, A., Ueda, S., and Ishihama, A. (1999) Growth phase-dependent variation in the protein composition of *Escherichia coli* nucleoid, *J. Bacteriol. 181*, 6361−6370.
50. Lipton, M. S., Pasa-Tolic, L., Anderson, G. A., Anderson, D. A., Auberry, D. A., Battista, J. R., Daly, M. J., and Fredrickson, J., et al., (2002) Global analysis of the *Deinococcus radiodurans* proteome by using accurate mass tags, *Proc. Natl. Acad. Sci. U.S.A. 99*, 11049−11054.
51. Harmon, F. G., and Kowalczykowski, S. C. (1998) Rec Q helicase, in concert with RecA and SSB proteins, initiates and disrupts DNA recombination, *Genes Dev. 12*, 1134−1144.
52. Marakova, K. S., Aravind, L., Wolf, Y. I., Tatusov, R. L., Minton, K. W., Koonin, E. V., and Daly, M. J. (2001) Genome of the extremely radiation-resistant bacterium *Deinococcus radiodurans* viewed from the perspective of comparative genomics, *Microbiol. Mol. Biol. Rev. 65*, 44−79.

BI0514010